Nuclear Physics A459 (1986) 387-416
North-Holland, Amsterdam

CONSISTENT CLUSTER MODEL DESCRIPTION OF THE ELECTROMAGNETIC PROPERTIES OF LITHIUM AND BERYLLIUM NUCLEI*

T. MERTELMEIER[1] and H.M. HOFMANN

Institut für Theoretische Physik der Universität Erlangen-Nürnberg, D-8520 Erlangen, West Germany

Received 12 November 1985
(Revised 16 May 1986)

Abstract: We calculate the electromagnetic properties of lithium and beryllium nuclei within a resonating group model using bare charges and g-factors. For ^{6}Li we give results for reduced transition strengths and explain the tiny quadrupole moment. For ^{7}Li and ^{7}Be we compute electromagnetic moments and transitions between bound states. Furthermore we reproduce the existing data on the radiative captures ^{3}He$(\alpha, \gamma)^7$Be and ^{3}H$(\alpha, \gamma)^7$Li. In the ^{7}Li case the calculations indicate an increase of the astrophysical S-factor for decreasing energy which might have astrophysical consequences. We show that closed channels do not influence results on the astrophysical S-factor at low energy. Finally we demonstrate that the polarisability of ^{7}Li originates from the virtual break-up at low energies. In this case, the ^{6}Li + n channels contribute appreciably.

1. Introduction

Within the last few years an increasing interest has been taken in the radiative capture reaction ^{3}He$(\alpha, \gamma)^7$Be at astrophysically low energies. This reaction and the determination of its astrophysical S-factor at zero energy was considered as the key to the solar neutrino puzzle [1]. In the meantime a lot of cross-section data for this capture reaction [2-7]) exists at low energies. But, since astrophysically small energies are inaccessible to laboratory measurements theoretical calculations are necessary, in order to extrapolate to these energies.

The capture reaction we are dealing with was investigated phenomenologically with the direct capture model [8-10]), which takes only the asymptotic parts of the wave functions into consideration. Using this one obtains the experimentally found energy dependence of the S-factor but not its absolute magnitude. The most recent phenomenological description was given by Buck *et al.* [11]), who describe ^{7}Li(^{7}Be) in terms of elementary ^{4}He and ^{3}H(^{3}He) particles which interact via an effective interaction. The parameters of this interaction are fixed by resonance positions and

* Supported by the Deutsche Forschungsgemeinschaft, Bonn and by the Bundesministerium für Forschung und Technologie, Bonn, West-Germany.

[1] Present address: Fachbereich Physik, Universität Marburg, D-3550 Marburg, West-Germany.

electromagnetic quantities. The astrophysical S-factor is then calculated absolutely from the given relative motion wave function, neglecting all antisymmetrization effects.

Microscopic approaches based on the resonating group method (RGM) have been carried through by Kanada, Liu, Tang, and Walliser [12,13]) and Kajino and Arima [14]). In both models the parameters of the nucleon-nucleon potential are chosen in such a way as to reproduce those quantities which are important for the description of the radiative capture. Both groups take only the $\alpha + {}^3\mathrm{He}$ cluster decomposition into account.

Another motivation to be engaged in the calculation of the electromagnetic ground state properties of light nuclei are Coulomb-excitation studies [15-17]). Sub-Coulomb scattering of aligned ^{7}Li nuclei off heavy ions [18,19]) is a precise measure to determine the quadrupole moment, reduced transition strengths to excited states, and the polarisability of ^{7}Li via virtual excitation of high-lying states. The determination of the quadrupole moment of the nuclear ground state, however, is closely related to that of the transition strengths and the polarisabilities. This direct measurement of the quadrupole moment is independent of the atomic wave function necessary in hyperfine structure experiments. Vice versa the known nuclear quadrupole moment can be used to reliably determine electric field gradients and to check the quality of chemical calculation procedures [20,21]).

In this paper we investigate the radiative capture and the electromagnetic properties using a multichannel resonating group method which allows for studying the influence of inelastic channels and distortion effects, too. We employ an effective nucleon-nucleon potential without free parameters which can be used to describe many different nuclei [22,23]). In general, the RGM should be ideally suited to describe electromagnetic properties and photonuclear reactions of light nuclei emphasizing a marked cluster structure. On the other hand the refined RGM had been applied with great success to nuclear scattering and reactions [23]). In this paper we show for the first time that this method is also appropriate to describe the electromagnetic properties of light nuclei, which are very sensitive to the asymptotic parts of the wave functions.

In sect. 2 we present the electromagnetic multipole operators and the physical observables. The nuclear model is introduced in sect. 3, together with an outline of the procedure how to calculate the matrix elements of the electromagnetic one-particle operators. Sect. 4 is devoted to a presentation of the results concerning bound state properties of ^{6}Li, ^{7}Li, and ^{7}Be. Furthermore the radiative capture reactions $^3\mathrm{He}(\alpha, \gamma)^7\mathrm{Be}$ and $^3\mathrm{H}(\alpha, \gamma)^7\mathrm{Li}$ and the polarisability of ^{7}Li are discussed.

2. Electromagnetic multipole operators and physical observables

Due to the weakness of the interaction of the electromagnetic radiation field with a nuclear system as compared to the strength of the nuclear forces the necessary

transition probabilities can be calculated using Fermi's golden rule [24]). Involving a multipole expansion of the electromagnetic field the transition operators in the long wavelength limit are given by [25]):

$$O(\mathrm{E}, L\mu) = \sum_{j=1}^{A} e g_{lj} r_j^L Y_{L\mu}(\hat{\boldsymbol{r}}_j)\,, \tag{1}$$

$$O'(\mathrm{E}, L\mu) = -\sum_{j=1}^{A} g_{sj} \frac{e}{2mc} \frac{k}{L+1} \boldsymbol{L}(r_j^L Y_{L\mu}(\hat{\boldsymbol{r}}_j)) \cdot \boldsymbol{S}_j \tag{2}$$

$$O(\mathrm{M}, L\mu) = \sum_{j=1}^{A} 2 g_{lj} \frac{e}{2mc} \frac{1}{L+1} \boldsymbol{\nabla}(r_j^L Y_{L\mu}(\hat{\boldsymbol{r}}_j)) \cdot \boldsymbol{l}_j \tag{3}$$

$$O'(\mathrm{M}, L\mu) = \sum_{j=1}^{A} g_{sj} \frac{e}{2mc} \boldsymbol{\nabla}(r_j^L Y_{L\mu}(\hat{\boldsymbol{r}}_j)) \cdot \boldsymbol{S}_j\,. \tag{4}$$

The operators $O(\mathrm{E}, L\mu)$ and $O(\mathrm{M}, L\mu)$ give the interaction of the orbital angular momenta $\boldsymbol{l}_j$, the operators $O'(\mathrm{E}, L\mu)$ and $O'(\mathrm{M}, L\mu)$ that of the spins $\boldsymbol{S}_j$ of A nucleons with the electromagnetic field. The multipolarity of the transition is denoted by L and μ, the electric operators are marked by the letter E, the magnetic operators by M. The angular momentum operator $\boldsymbol{L}$ is given by $\boldsymbol{L} = -i\boldsymbol{r} \times \boldsymbol{\nabla}$. For the g-factors we use those of free nucleons, i.e. $g_l(\text{proton}) = 1$, $g_l(\text{neutron}) = 0$, $g_s(\text{proton}) = 5.586$, and $g_s(\text{neutron}) = -3.826$. The mass of the nucleon is denoted by m, and k is the wave vector of the photon. The operators (1) to (4) are written in a translational invariant form because the one-particle coordinates $\boldsymbol{r}_j$ denote the space coordinates in the center-of-mass (c.m.) frame of the A nucleons. This choice is appropriate especially if one describes the nuclear system with a resonating group method and is most important for light nuclei to avoid spurious CM-excitations. In deriving the formulae (1) to (4) the long wave limit has been applied because we are only interested in transitions for which the wave length $1/k$ of the photon is much larger than the spatial extension of the nuclear system. This condition is well fulfilled for transitions between low-lying states in the nuclei considered.

The electric orbital operator (1) stems from Siegert's theorem [26]). Hence this operator includes the most part of the meson exchange currents, whereas the other operators do not [27]).

The physical observables we are interested in may be expressed by these four multipole operators. The aim is a consistent description of the electromagnetic bound state properties like moments and transition strengths as well as quantities involving scattering states, i.e. the radiative capture cross section and the polarisability of ^{7}Li due to the virtual break-up. To make this paper self-contained we present the necessary observables in the following.

Consider an electric or magnetic transition of multipolarity L between the two bound states $|\alpha J\rangle$ and $|\alpha' J'\rangle$ where J denotes the total angular momentum and α

all further quantum numbers of the state. The reduced transition strength is given by

$$B(\overset{\mathrm{E}}{\mathrm{M}}L, \alpha] \to \alpha' J') = |\langle \alpha' J' \| O(\overset{\mathrm{E}}{\mathrm{M}}, L) + O'(\overset{\mathrm{E}}{\mathrm{M}}, L) \| \alpha J \rangle|^2/(2J+1)\,, \tag{5}$$

which is the nuclear structure dependent part of the gamma width. For the reduced matrix elements $\langle \alpha' J' \| O(L) \| \alpha J \rangle$ the convention of Edmonds [28]) is used.

The electric quadrupole moment Q is proportional to the expectation value of the E2 operator in the state $|\alpha J J_z = J\rangle$

$$Q = \sqrt{\tfrac{16}{5}\pi}\langle \alpha JJ | O(\mathrm{E}, 20) | \alpha JJ \rangle\,. \tag{6}$$

The magnetic dipole moment is given by

$$\mu = \sqrt{\tfrac{4}{3}\pi}\langle \alpha JJ | O(\mathrm{M}, 10) + O'(\mathrm{M}, 10) | \alpha JJ \rangle\,, \tag{7}$$

and analogously, for the magnetic octupole moment Ω we define

$$\Omega = \sqrt{\tfrac{4}{5}\pi}\langle \alpha JJ | O(\mathrm{M}, 30) + O'(\mathrm{M}, 30) | \alpha JJ \rangle\,. \tag{8}$$

For the radiative capture we will calculate the angle-integrated partial cross section

$$\begin{aligned}\sigma(L, \alpha L_{\mathrm{rel}} S_c J \to \alpha' J') &= (8\pi/\hbar v)[(L+1)/L((2L+1)!!)^2]k^{2L+1}/((2S_c+1)(2L_{\mathrm{rel}}+1)) \\ &\times |\langle \alpha L_{\mathrm{rel}} S_c J \| O(\overset{\mathrm{E}}{\mathrm{M}}, L) + O'(\overset{\mathrm{E}}{\mathrm{M}}, L) \| \alpha' J' \rangle|^2\,,\end{aligned} \tag{9}$$

which describes the emission of a photon of multipolarity L and wave vector k from the scattering partial wave with relative angular momentum L_{rel} between the two fusing nuclei, channel spin S_c, and relative velocity v. The initial scattering function contains an incoming Coulomb wave moving along the z-axis and is flux-normalized.

In order to study the capture reaction at astrophysically low energies it is convenient to define the S-factor [1])

$$S(E) = \sigma(E) E \exp(2\pi Z_1 Z_2 e^2/\hbar v) \tag{10}$$

which shows an energetically smooth behaviour and which contains the nuclear physics information because kinematic and Coulomb barrier penetration factors have been eliminated. E denotes the relative motion energy ($E = \frac{1}{2}mv^2$) and $\sigma(E)$ is the sum of all partial contributions (9) to the radiative capture cross section.

A further topic of this paper is the investigation of the electric polarisability of the nucleus ^{7}Li appearing in the sub-Coulomb scattering off heavy nuclei, ^{58}Ni or ^{120}Sn for instance [18,19]).

The semi-classical theory of Coulomb excitation [29]) shows that the deviation from the Rutherford cross section is dominated by the ground state reorientation effect and by the real E2 excitation to the first excited state. Additionally, the polarisability of ^{7}Li in the Coulomb field of the target caused by the virtual E1 excitation can be extracted from the experimental data for the scattering of polarised ^{7}Li as a higher order effect.

Within the limits of an adiabatic approximation [29]) these virtual dipole excitations are taken into consideration [30]) by an effective polarisation potential [19])

$$V_{\mathrm{pol}} = -\tfrac{1}{2}Z^2e^2\alpha/r^4 - (\tfrac{9}{5}\pi)^{1/2}(Z^2e^2/r^4)\tau_{\mathrm{if}}Y_{20}(\hat{\boldsymbol{J}}\cdot\hat{\boldsymbol{r}}) \tag{11}$$

where $\hat{\boldsymbol{J}}$ is the direction of the polarisation. The charge of the collision partner is denoted by Z, and the polarisability α of the ^{7}Li nucleus is defined as

$$\alpha = \tfrac{8}{9}\pi \sum_{\lambda} \int \mathrm{d}E |\langle \lambda E J_\lambda \| O(\mathrm{E1}) \| J_i \rangle|^2 / ((E - E_i)(2J_i + 1)) \,. \tag{12}$$

Here the continuum states $|\lambda E J_\lambda\rangle$ are normalised to a δ-function in the energy and the integration extends from the threshold energy of the channel λ up to infinity. (Note that conventionally all expressions for the polarisability are just given by transitions between discrete levels [15,30,31]).)

There are several possibilities to give an expression for the tensor moment τ_{if} of the polarisability. One possibility is the connection to the inversely energy-weighted dipole sum $S_{\mathrm{if}}(\mathrm{E1})$, introduced in ref. [15]):

$$\tau_{\mathrm{if}}(S_{\mathrm{if}}(\mathrm{E1})) = \tfrac{8}{9}\pi(\tfrac{10}{3})^{1/2} S_{\mathrm{if}}(\mathrm{E1}) \tag{13}$$

with

$$S_{\mathrm{if}}(\mathrm{E1}) = (-1)^{-J_i - J_f} \sum_{\lambda} \begin{Bmatrix} 1 & 1 & 2 \\ J_f & J_i & J_\lambda \end{Bmatrix} \times \int \mathrm{d}E \langle J_i \| O(\mathrm{E1}) \| \lambda E J_\lambda \rangle \langle \lambda E J_\lambda \| O(\mathrm{E1}) \| J_f \rangle / (E - E_i) \,. \tag{14}$$

Within the semi-classical approach, for a deformed nucleus this tensor part of the polarisation potential may be alternatively expressed [29]) by the polarisability α and a deformation parameter $\alpha_{\mathrm{if}}^{20}$:

$$\tau_{\mathrm{if}}(\alpha) = (5/9\pi)^{1/2} \alpha \alpha_{\mathrm{if}}^{20} \tag{15}$$

where the deformation parameter is defined as

$$\alpha_{\mathrm{if}}^{20} = 4\pi \langle J_i \| O(\mathrm{E2}) \| J_f \rangle / 3ZeR_0^2 \,. \tag{16}$$

In this expression R_0 is a typical nuclear radius ($R_0 = 1.2\,\mathrm{fm} \cdot A^{1/3}$).

Usually [31]) one aims at avoiding a complicated scattering calculation and assumes that the total E1 strength would be concentrated in a narrow energy range, i.e. all intermediate states would have the same energy E_{D}. With the help of the completeness of the intermediate states this closure approximation leads immediately to the expressions [31])

$$\tau_{\mathrm{if}}^{\mathrm{cl}}(S_{\mathrm{if}}(\mathrm{E1})) = \tfrac{8}{9}\pi \cdot (\tfrac{2}{3})^{1/2} \langle J_i \| T(2) \| J_f \rangle / E_{\mathrm{D}} \,, \tag{17}$$

$$\tau_{\mathrm{if}}^{\mathrm{cl}}(\alpha) = -(\tfrac{5}{3}\pi)^{1/2} \langle J_i \| T(0) \| J_i \rangle \alpha_{\mathrm{if}}^{20} / (E_{\mathrm{D}}(2J_i + 1)) \,. \tag{18}$$

The two-particle operator $T(kq)$ can be expressed by the electric dipole operator and is given by [31])

$$T(kq) = \sum_m (1m1q-m|kq) O(\mathrm{E}1m) O(\mathrm{E}1q-m)$$

$$= [O(\mathrm{E}1) \otimes O(\mathrm{E}1)]^{kq}, \qquad k = 0, 2. \tag{19}$$

In sect. 4 we will compare the various expressions for the tensor polarisability τ (eqs. (13)-(18)) and discuss the validity of the underlying model assumptions.

For all physical observables we are dealing with we need the matrix elements of the electromagnetic multipole operators respectively of the operators $T(kq)$ [eq. (19)], calculated either with bound state wave functions or with one bound state and one scattering wave function. In the next section we will give the ansatz for the wave functions and present the method of calculating the matrix elements.

3. The wave functions and the calculation of the matrix elements

The underlying nuclear model we use is the refined resonating group model (RRGM) initiated by Hackenbroich [32,33]). It is ideally suited to the description of scattering and reactions involving light complex nuclei [22]) and allows for coupled channel calculations. In this paper we show for the first time that this model is also qualified for the calculation of electromagnetic transitions and photonuclear reactions where one probes the wave functions beyond the nuclear interaction range because of the long range nature of the electromagnetic force. In all investigations we use the same effective nucleon-nucleon potential, given in appendix 3, which contains central, spin-orbit, and tensor forces, and the Coulomb potential.

The bound state and scattering functions are obtained in a unified way by a variational calculation. The bound state wave functions are determined by the Ritz variational principle. Their orbital part contains gaussians and solid spherical harmonics. Details are given elsewhere [35]).

The determination of the two-fragment scattering wave function is based on the Kohn-Hulthén variational principle [33]). The two-fragment scattering function with an incoming Coulomb wave in channel λ and with channel spin S_λ, M_λ is given by the expression

$$|\lambda S_\lambda M_\lambda\rangle = \sum_{L_\lambda=0}^{\infty} \sqrt{4\pi(2L_\lambda+1)}\, i^{L_\lambda}\, \mathrm{e}^{i\sigma_{L_\lambda}} \sum_{Jj} (L_\lambda 0 S_\lambda M_\lambda | Jj)$$

$$\times \mathscr{A}\Bigg\{ \sum_\tau ((\mathbb{1}-ia)^{-1})_{\lambda\tau} \sum_\kappa \Bigg(\delta_{\tau\kappa} F_{L_\kappa}(R_\kappa) + a_{\tau\kappa} \tilde{G}_{L_\kappa}(R_\kappa) + \sum_m b_{\tau\kappa m} E_{\kappa m}(R_\kappa) \Bigg)$$

$$\times [Y_{L_\kappa}(\hat{\boldsymbol{R}}_\kappa)/K_\kappa R_\kappa \otimes [\Psi_\kappa^{J_1\pi_1} \otimes \psi_\kappa^{J_2\pi_2}]^{S_\kappa}]^{J_j} \Bigg\} \tag{20}$$

where σ_{L_λ} denotes the Coulomb phase shift. The functions F_{L_κ} are regular Coulomb

waves, $\tilde{G}_{L_\kappa}$ are regularized[35]) irregular Coulomb waves, and $E_{\kappa m}$ are square-integrable functions of the type $R_\kappa^{L_\kappa+1}\exp(-\delta_{\kappa m}R_\kappa^2)$ which allow for distortion effects in the interaction region. The relative motion coordinate between the two fragments in channel κ is denoted by $\boldsymbol{R}_\kappa$. The elements $a_{\tau\kappa}$ of the reactance matrix a and the coefficients $b_{\tau\kappa m}$ are the variational parameters. The internal functions $\psi_\kappa^{J_i^{\pi_i}}$ $(i=1,2)$ are the bound states of the two fragments, whose spins J_1 and J_2 are coupled to the channel spin S_κ, which is then coupled with the relative angular momentum L_κ to the total J with z-projection j. The functions $|\lambda L_\lambda S_\lambda J\rangle$ in the radiative capture cross section formula of eq. (9) are related to the ones introduced in eq. (20) by:

$$|\lambda S_\lambda M_\lambda\rangle=\sum_{L_\lambda Jj}(L_\lambda 0 S_\lambda M_\lambda|Jj)|\lambda L_\lambda S_\lambda Jj\rangle\,. \tag{21}$$

If we are dealing with only one channel (with channel spin S_c, M_c and relative angular momentum $L_{\rm rel}$, reactance matrix $a=\tan\delta_{\rm rel}$), the scattering function (20) reduces for large spatial separations of the fragments to

$$|S_cM_c\rangle\xrightarrow{R\to\infty}\sum_{L_{\rm rel}}\sqrt{4\pi(2L_{\rm rel}+1)}\,i^{L_{\rm rel}}\,e^{i(\sigma_{L_{\rm rel}}+\delta_{L_{\rm rel}})}$$
$$\times(\cos\delta_{L_{\rm rel}}F_{L_{\rm rel}}(R)+\sin\delta_{L_{\rm rel}}G_{L_{\rm rel}}(R))(Y_{L_{\rm rel}0}(\hat{\boldsymbol{R}})/KR)[\psi^{J_1\pi_1}\otimes\psi^{J_2\pi_2}]^{S_cM_c} \tag{22}$$

where $\delta_{L_{\rm rel}}$ is the nuclear phase shift.

In the RRGM the variational equations are solved algebraically, because the Coulomb functions in the interaction region are approximated by the square-integrable functions $E_{\kappa m}$ $(m=1,\ldots,20)$ with the parameters $\delta_{\kappa m}$ taken as[36])

5.0, 1.7, 0.7, 0.35, 0.15, 0.07, 0.04, 0.025, 0.015, 0.01, 0.007, 0.005, 0.0035, 0.0025, 0.0015, 0.001, 0.0007, 0.0004, 0.0002, 0.0001 in units of $\rm fm^{-2}$.

Hence, the bound state wave functions as well as the scattering functions can be written as

$$\mathcal{A}(\psi^{Jj})=\mathcal{A}\sum_{\alpha m\sigma}c_\alpha^{lSJ}(lmS\sigma|Jj)|\alpha lm\rangle|\alpha S\sigma\rangle \tag{23}$$

where l, S and J denote the orbital angular momentum, the total spin and the total angular momentum and m, σ and j their z-projections. The symbol α stands for all other quantum numbers and for possibly different cluster decompositions or different gaussian functions for the description of the fragments.

Hence, the calculation of matrix elements of the electromagnetic operators [eqs. (1)–(4)] with bound and scattering wave functions is reduced to the calculation of these matrix elements with functions of the type (23). Since the particles within a cluster are in relative S-states only, the orbital part $|\alpha lm\rangle$ is invariant under permutations which exchange particles only within clusters.

In the following we will describe the method of calculating the matrix elements of the one-particle operators O (1)-(4)

$$\langle \psi^{J'j'} | \mathscr{A} O | \psi^{Jj} \rangle$$

where the antisymmetrizer is the sum over all permutations P of A particles including the sign:

$$\mathscr{A} = \sum_{P \in S_A} \operatorname{sgn} P P .$$

This task will be tackled in three steps. First, the electromagnetic multipole operators are split up into spherical tensor operators in coordinate and spin space. The operators (1) to (4) are given explicitly in this form in ref. [36]).

In the second step for each permutation the calculation of the spin matrix element is performed. This is rather straightforward, because the spin operators are for the orbital interactions (1) and (3) the identity in spin space, and for the spin interactions (2) and (4) the spin operators S_j of the jth nucleon. Furthermore, the spin functions are superpositions of products of one-particle spin-isospin functions, so that the application of the spin operators is quite obvious. For those permutations, which give the same coordinate space matrix element due to the cluster symmetry of the orbital wave function $|\alpha lm\rangle$ the spin matrix elements are summed up [32]).

The last and most complicated step consists in the calculation of the coordinate space matrix elements themselves. The method is based on the calculation of the norm matrix elements given by Hackenbroich [32]). In order to make this paper self-contained we recapitulate the essential steps in the following. With the notation used in refs. [32,35]), the norm matrix element for a fixed permutation P is given by

$$\begin{aligned} \langle \alpha' l' m' | P \alpha l m \rangle &\sim \Gamma_{L_1 M_1 \cdots L_N M_N} \\ &= \int \mathrm{d}\boldsymbol{s}_1 \cdots \mathrm{d}\boldsymbol{s}_{A-1} \exp\left(- \sum_{\nu,\mu=1}^{A-1} \rho_{\nu\mu} \boldsymbol{s}_\nu \cdot \boldsymbol{s}_\mu \right) \prod_{n=1}^{N} \mathscr{Y}_{L_n M_n}(\boldsymbol{Q}_n) \end{aligned} \tag{24}$$

where the $\mathscr{Y}_{L_n M_n}$ are solid spherical harmonics. Here the one-particle coordinates $\boldsymbol{r}_i$ $(i = 1, \ldots, A)$, which are found in the wave functions are expressed by the Jacobi coordinate vectors $\boldsymbol{s}_\nu$ $(\nu = 1, \ldots, A-1)$, say of the left-hand side wave function. Because of the translational invariance of the cluster model the integrals do not depend on the Jacobi coordinate vector $\boldsymbol{s}_A$, which is proportional to the center-of-mass vector. The vectors $\boldsymbol{Q}_n$ between clusters are linear combinations of the $\boldsymbol{s}_\nu$, depending on the considered permutation P and the cluster decomposition. The number N is the number of angular momenta in the bra and ket functions, i.e.

$$N = n_\ell + n_r - 2$$

with n_ℓ and n_r denoting the number of clusters in bra and ket. L_n and M_n stand for the angular momenta and their z-projections in the wave functions and $\rho_{\nu\mu}$ results from expressing the gaussians of the wave functions in terms of the Jacobi coordinates.

Using the generating function of the spherical harmonics [37])

$$(\mathbf{\Lambda}(b)\cdot\boldsymbol{r})^l = b^l \sum_{m=-l}^{l} C_{lm} b^{-m} \mathcal{Y}_{lm}(\boldsymbol{r}) \tag{25}$$

with the vector

$$\mathbf{\Lambda}(b) = (1-b^2,\ i+ib^2,\ -2b) \tag{26}$$

and

$$C_{lm} = (-2)^l l! \sqrt{4\pi/(2l+1)(l-m)!(l+m)!}\,, \tag{27}$$

we consider the generating integral

$$I(a_1, b_1, \ldots, a_N, b_N) = \int \mathrm{d}\boldsymbol{s}_1 \cdots \mathrm{d}\boldsymbol{s}_{A-1} \exp\left(- \sum_{\nu,\mu=1}^{A-1} \rho_{\nu\mu} \boldsymbol{s}_\nu \cdot \boldsymbol{s}_\mu + \sum_{u=1}^{N} a_n \mathbf{\Lambda}(b_n)\cdot \mathbf{Q}_n \right). \tag{28}$$

This is expanded in powers of the parameters $a_1, b_1, \ldots, a_N, b_N$. The result

$$I(a_1, b_1, \ldots, a_N, b_N) = \sum_{l_1 m_1 \cdots l_N m_N} \prod_{n=1}^{N} (C_{l_n m_n}/l_n!) a_n^{l_n} b_n^{l_n - m_n} \Gamma_{l_1 m_1 \cdots l_N m_N} \tag{29}$$

contains the desired integrals as expansion coefficients besides known numerical factors.

On the other hand, eq. (28) may be integrated explicitly by diagonalizing the quadratic form $(\rho_{\nu\mu})$ and employing the method of completing squares. This result can be expanded again in powers of $a_1, \ldots, b_N$. Equating the expansion coefficients determines the desired norm integrals. Explicit expressions of these norm integrals are given elsewhere [32,35]).

In the following we will show that the coordinate space matrix elements of the transition operators can be reduced to a sum of such norm integrals. Employing the Wigner-Eckart theorem [28]) it is sufficient to calculate matrix elements with $m = l$ and $m' = l'$, i.e. $\langle \alpha' l' l' | P w_i | \alpha l l \rangle$, where w_i is the orbital part of the multipole operators; P denotes the permutation and i the interacting particle.

For both electric operators, w_i is given by [36])

$$w_i(Lq) = \mathcal{Y}_{Lq}(\boldsymbol{r}_i)\,, \tag{30}$$

see also eq. (1). Therefore the orbital matrix elements are written as

$$\begin{aligned}
&\langle \alpha' l' l' | P w_i(Ll'-l) | \alpha l l \rangle \\
&\quad \sim \Gamma_{L_1 M_1 \cdots L_N M_N}(i, P, \mathrm{E}L) \\
&\quad = \int \mathrm{d}\boldsymbol{s}_1 \cdots \mathrm{d}\boldsymbol{s}_{A-1} \exp\left(- \sum_{\nu\mu}^{A-1} \rho_{\nu\mu} \boldsymbol{s}_\nu \cdot \boldsymbol{s}_\mu \right) \left(\prod_{n=1}^{N} \mathcal{Y}_{L_n M_n}(\boldsymbol{Q}_n) \right) \mathcal{Y}_{Ll'-l}(\boldsymbol{Q}_{N+1})\,.
\end{aligned} \tag{31}$$

Here the operator w_i $(Ll'-l)$ [eq. (30)] is responsible for the additional term $\mathcal{Y}_{Ll'-l}(\boldsymbol{Q}_{N+1})$, where the vector $\boldsymbol{Q}_{N+1}$ is just the permuted one-particle coordinate $\boldsymbol{r}_{P(i)}$ and has to be expressed as a linear combination of the Jacobi coordinates. Consequently, these integrals are of the same type as the norm integral except for the fact that the number of spherical harmonics (and accordingly the number of generating parameters a_n and b_n) are enlarged by one:

$$\Gamma_{L_1M_1\cdots L_NM_N}(i, P, \mathrm{E}L) = \Gamma_{L_1M_1\cdots L_NM_NLl'-l}\,. \tag{32}$$

The same is true also for the magnetic spin operator (eq. 4), for which the orbital part w_i of the operator is given by $\mathcal{Y}_{L-1q}$, hence analogously to eq. (32) the matrix element is given by the same expression with only L replaced by $L-1$.

The coordinate space part of the magnetic orbital operator (3), however, contains a differential operator acting on the wave function, see eq. (3), and is given by

$$\tilde{w}_i(L\mu) = \sum_{qq'} (Lq1q'|L\mu)\mathcal{Y}_{Lq}(\boldsymbol{r}_i)\nabla_i(q')\,. \tag{33}$$

In appendix 1 it is shown that the integral again can be expressed by norm integrals

$$\begin{aligned}
&\Gamma_{L_1M_1\cdots L_NM_N}(i, P, \mathrm{M}L)\\
&= \sum_{n=1}^{N+1} K_n(L_n/C_{L_nM_n})\\
&\times\{\sqrt{2}\,C_{L_n-1M_n+1}(Ll'-l-111|Ll'-l)\Gamma_{L_1M_1\cdots L_n-1M_n+1\cdots L_NM_NLl'-l-1}\\
&-2C_{L_n-1M_n}(Ll'-l10|Ll'-l)\Gamma_{L_1M_1\cdots L_n-1M_n\cdot L_NM_NLl'-l}\\
&+\sqrt{2}\,C_{L_n-1M_n-1}(Ll'-l+11-1|Ll'-l)\Gamma_{L_1M_1\cdots L_n-1M_n-1\cdots L_NM_NLl'-l+1}\}
\end{aligned} \tag{34}$$

where the quantities K_n are defined in eq. (A.11). Thus, we reduced these matrix elements to a sum of norm integrals containing one additional angular momentum. The consequence of the differential operators is that in the summation over n the nth angular momentum L_n is diminished by 1.

Analogously, the matrix elements of the two-particle operator $T(kq)$, which are required for the electric polarisability in the closure approximation [eqs. (17)-(19)], can be expressed directly by norm integrals containing however two more angular momenta. These arise from the two E1 operators which are coupled to $T(kq)$, $(k=0, 2)$.

With the help of eqs. (31)-(34) and analogous ones for the two-body operators, we can calculate all physical observables introduced in sect. 2 for the wave functions discussed in this chapter. In the sequel we will present the results and discuss them.

4. Results and discussion

The concepts illustrated so far are now applied to give a consistent description of electromagnetic properties of light nuclei. We consider ground state properties like radius, electric quadrupole moment and magnetic dipole moment of ^{6}Li, ^{7}Li and ^{7}Be, and electromagnetic transitions between low-lying states in these nuclei. Furthermore we calculate the cross section for the radiative capture reactions ^{3}He$(\alpha, \gamma)^7$Be and ^{3}H$(\alpha, \gamma)^7$Li at small energies. Finally we investigate the electric polarisability of ^{7}Li. Although all these quantities are not independent of each other, we will present them in a consecutive manner, but nevertheless refer in a particular section to the others mutually.

4.1. MULTIPOLE MOMENTS AND ELECTROMAGNETIC TRANSITIONS

Let us first consider the case of the nucleus ^{6}Li. If we start with the simple ansatz for the ^{6}Li wave function consisting only of a two-cluster function, namely the alpha and the deuteron, with relative angular momentum $L_{\text{rel}} = 0$, then this ^{6}Li would have no electric quadrupole moment in contrast to the experimental value of $Q(^6\text{Li}) = -0.06\, e \cdot \text{fm}^2$ (cf. table 1).

An additional D-wave on the relative motion would give $Q(^6\text{Li}) = -1 e \cdot \text{fm}^2$, a value way in excess of the experimental one.

TABLE 1

Comparison of the calculated electromagnetic properties of ^{6}Li with the experimental data (μ_k is the nulcear magneton)

^{6}Li	Calc.	Exp.	Ref.
r_c (fm)	2.40	2.54 ± 0.06 2.56 ± 0.05 2.57 ± 0.10	[41]
$Q(e \cdot \text{fm}^2)$	−0.076	-0.0644 ± 0.0007	[40]
μ/μ_k	0.83	0.822	[40]
$B(\text{E2}, 3^+ \to 1^+)(e^2 \cdot \text{fm}^4)$	10.1	10.9 ± 2.1	[40]
$B(\text{E4}, 3^+ \to 1^+)(e^2 \cdot \text{fm}^8)$	7.0		
$B(\text{M3}, 3^+ \to 1^+)(\mu_k^2 \cdot \text{fm}^4)$	91		
$B(\text{E2}, 2^+ \to 1^+)(e^2 \cdot \text{fm}^4)$	17	4.7 ± 1.5 10.8 ± 1.1	[39,40] [42]
$B(\text{M1}, 2^+ \to 1^+)(\mu_k^2)$	0.7×10^{-4}		
$B(\text{M3}, 2^+ \to 1^+)(\mu_k^2 \cdot \text{fm}^4)$	125		
$B(\text{E2}, 1^{+*} \to 1^+)(e^2 \cdot \text{fm}^4)$	23		
$B(\text{M1}, 1^{+*} \to 1^+)(\mu_k^2)$	2×10^{-4}		

On the other hand, for a three-cluster wave function consisting of an alpha particle, a proton and a neutron with S- and D-wave between them the resulting ^{6}Li would have a positive quadrupole moment because of the positive quadrupole moment of the deuteron build in.

Therefore, a reasonable description of the electromagnetic properties of this nucleus cannot be obtained unless a three-cluster wave function with S- and D-waves on both cluster relative coordinates is used, which is also found in ref. [38])*. These wave functions for the ground state of ^{6}Li($J^\pi = 1^+$, $T = 0$) and the excited $T = 0$ − triplet ($J^\pi = 3^+, 2^+, 1^+$) are given in appendix 2.

In table 1 we compare the calculated quantities and measured values for the charge radius r_c, the electric quadrupole moment Q, the magnetic dipole moment μ and the various B-values for the transitions to the ground state. The calculated quadrupole moment agrees well with the tiny experimental value and is the outcome of the destructive interference of the two D-waves. The agreement of the $B(\mathrm{E2}, 3^+ \to 1^+)$ value with the data is excellent. The $B(\mathrm{E2}, 2^+ \to 1^+)$ value is reasonable reproduced too, if one realizes that the 2^+ state is rather high lying and the background is not well known for the interpretation of the data [39]). Furthermore this state is already above the three-particle threshold ^{4}He + n + p, and therefore the ansatz for the wave function might be too simple.

The seven-nucleon systems ^{7}Li and ^{7}Be are well represented by two-cluster wave functions (^{4}He + ^{3}H/^{3}He) with relative angular momentum $L_{\mathrm{rel}} = 1$. The coupling of L_{rel} with the spin $S = \frac{1}{2}$ of the ^{3}H/^{3}He-nucleus yields the ground state dublett with $J^\pi = \frac{3}{2}^-$ and $\frac{1}{2}^-$. The wave functions of this two-cluster type are given in appendix 2. The first version, called WF1, consists of one gaussian function only for the relative motion of the two clusters. The same gaussian is used for the ground and first excited state. For the wave function WF2 a variational procedure has been carried out for the excited state, too. In this case now the two states differ in the width of the gaussian function for the cluster relative motion.

The calculated electromagnetic properties of ^{7}Li are presented in table 2 together with the data. Whereas the electric quadrupole moment and the $B(\mathrm{E2}, \frac{3}{2}^- \to \frac{1}{2}^-)$ value are nicely reproduced, the magnetic properties are slightly underestimated. The reason for this is that the magnetic multipole operators as used do not take mesonic effects into account, quite contrary to the electric operator. The improved wave function WF2 for the excited state gives a $B(\mathrm{E2})$ value in very nice agreement with the most recent data [19,30]).

Since for the nucleus ^{7}Be almost no data exist, we show in table 2 only the predicted quantities calculated with the function WF1.

The bound state functions considered so far for the seven-nucleon system consist of only one gaussian function for the cluster relative motion. Hence, it is not surprising that these wave functions are not well suited to describe the radiative capture at very low energies because the asymptotic behaviour of this relative motion bound state function is not correct. The calculated charge radius, which is too small, is another indication of this fact.

* Note, that we count a deuteron with S- and D-waves as two clusters, whereas such a deuteron is counted as one cluster in ref. [38]).

TABLE 2

Electromagnetic properties of ^{7}Li and ^{7}Be, calculated with the wave functions WF1, WF2, WF3 and WF4, as explained in the text, and the experimental data

	^{7}Li						^{7}Be		
	WF1	WF2	WF3	WF4	exp	ref.	WF1	exp	ref.
r.m.s. (fm)	2.34		2.46	2.40			2.34		
r_c (fm)	2.27		2.38	2.31	2.55 ± 0.07	[43]	2.39		
					2.39 ± 0.03	[41]			
					2.41 ± 0.1				
Q ($e \cdot$ fm^2)	−3.71		−4.19	−3.42	$\lvert 3.8 \pm 1.1 \rvert$	[43]	−5.84		
					−4.1	[44]			
					-3.4 ± 0.6	[18]			
					-4.0 ± 1.1	[17]			
					-3.70 ± 0.08	[19,30]			
					-3.66 ± 0.03	[20]			
					−4.06	[21]			
μ (μ_k)	3.16		3.16	2.79	3.256	[40]	−1.27		
Ω ($\mu_k \cdot$ fm^2)	−10.5		−11.8	−10.8	$\lvert 7.5 \pm 1.6 \rvert$	[45]	7.21		
					$\lvert 9.3 \pm 0.4 \rvert$	[43]			
$B(\mathrm{E2}, \frac{3}{2}^- \to \frac{1}{2}^-)$ ($e^2 \cdot$ fm^4)	6.86	8.49	11.3	5.38	6.7 ± 0.2	[43]	17.0		
					7.4 ± 0.1	[16]			
					8.3 ± 0.6	[15]			
					7.42 ± 0.14	[17]			
					8.3 ± 0.5	[19,30]			
$B(\mathrm{M1}, \frac{3}{2}^- \to \frac{1}{2}^-)$ (μ_k^2)	2.17	1.96	2.10	2.15	2.48 ± 0.12	[43]	1.58	1.87 ± 0.25	[40]

This defect can be removed by increasing the number of gaussian functions for the relative cluster motion. Gaussian functions with small width parameters, corresponding to large separations of the clusters do almost not contribute to the binding energy. Therefore three gaussian functions suffice to determine the binding energy and further ones with smaller width parameters reproduce the asymptotic behaviour of the wave function. Furthermore, using the potentials employed in refs. [13,14]) and the internal wave functions of these references, we reproduce all quoted results to three leading digits when we expand the relative motion wave function into four gaussians. Therefore we consider four gaussian functions enough to approximate the bound state wave function. Such a wave function, called WF3, is given in appendix 2. Table 2 shows that for this function the calculated charge radius agrees with the experimental data within the error bars. On the other hand the electric quadrupole moment and the B(E2) value are overestimated because now the wave function reaches far more out. These too large values can be reduced (table 2) with a more complicated bound state wave function which consists not only of a ^{4}He+^{3}H-structure but contains also a ^{6}Li+n cluster decomposition. This wave function is called WF4; its parameters are given in appendix 2, too. We see that a ^{6}Li+n

admixture of about 10% results in a dramatic change of the quadrupole moment and of the $B(\mathrm{E2})$ value.

However, one should keep in mind that we are employing an effective nucleon-nucleon potential without free parameters. It is therefore no surprise that little modifications of the strength parameters of the potential allow to reproduce the electromagnetic data. A reduction of the spin-orbit force by 20% for instance leads to a quadrupole moment $Q = -3.67e \cdot \mathrm{fm}^2$ and to the reduced transition strength $B(\mathrm{E2}, \frac{3}{2}^- \to \frac{1}{2}^-) = 6.52e^2 \cdot \mathrm{fm}^4$, calculated with a wave function of the type WF4. Thus the electromagnetic properties might offer a possibility to favourably determine the parameters of the potential.

Returning to the wave function WF4, this function reproduces the cluster separation energy correctly and the asymptotic shape almost correctly, see fig. 1. For the calculation of the radiative capture cross section at low energies it is essential that both these quantities are reproduced well.

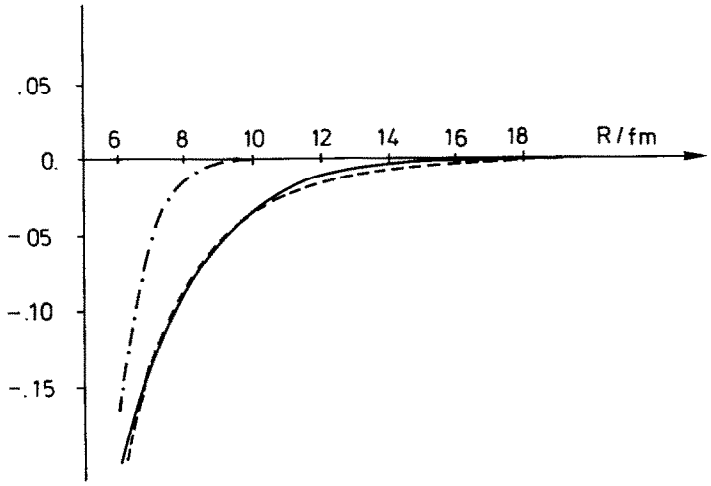

Fig. 1. The asymptotic behaviour of the radial parts of the wave function WF4 (full line) and of an Whittaker function with the same energy (dashed line) in arbitrary units. In addition the radial part of WF1 (dashed-dotted line) is shown, which falls off much too rapidly, hence the radiative capture results for low energy are grossly underestimated.

Summarizing the results for the electromagnetic moments and transitions for the Lithium isotopes we find that for ^{6}Li only a three-cluster wave function suffices, whereas for ^{7}Li already a rather simple cluster model wave function reproduces the data very well. If one aims however at a consistent description of other quantities too, which are sensitive to the asymptotic shape of the wave function, one has to

admix a ^{6}Li + n-structure to the simple ^{4}He + ^{3}H fragmentation in order to reproduce the separation energy.

4.2. THE CAPTURE REACTIONS ^{3}He(α, γ)^{7}Be AND ^{3}H(α, γ)^{7}Li

The fusion reaction ^{3}He(α, γ)^{7}Be plays a key-role for the nuclear physics aspect of the solar neutrino problem [1]). The E1 capture which is nearly the sole contribution may happen from the $^2S_{1/2}$, $^2D_{3/2}$ and $^2D_{5/2}$ partial waves leading to the $\frac{3}{2}^-$ ground state and from the $^2S_{1/2}$ and $^2D_{3/2}$ partial waves to the first excited $\frac{1}{2}^-$ state in ^{7}Be. In order to obtain a reasonable agreement with the experimental cross section data, the bound state wave function has to fulfill two conditions. First, the asymptotic behaviour of the radial motion has to be that of a Whittaker function [46]). This is achieved in taking a superposition of four gaussians for the relative motion function, which gives a good approximation to a Whittaker function at least up to 20 fm, see fig. 1.

Secondly, the bound state wave function must have the correct cluster separation energy, because otherwise the argument in the Whittaker function would be incorrect. Since we stick to the effective potential used for other nuclei already we can only meet the last requirement by admixing a ^{6}Li + p configuration. A wave function which satisfies all the above requirements is WF4, given in appendix 2. For the scattering wave function a simple $\alpha + {}^3$He wave which reproduces the positive parity phase shifts in the considered energy range suffices.

In fig. 2 the result for the E1 fusion cross section is compared with the existing data [2-6]). The dashed line gives the capture into the ground state and the full line the capture into the ground and first excited state of ^{7}Be. Not only for the cross section but also for the astrophysical S-factor which is shown in fig. 3, the agreement between theory and experiment is excellent. The branching ratio

$$R(E) = \sigma(^7\mathrm{Be}^*(\tfrac{1}{2}))/\sigma(^7\mathrm{Be}(\tfrac{3}{2}^-)) \tag{35}$$

is shown in fig. 4. It is almost energy independent and slightly larger than 0.4. In fig. 5 the relative contributions to the cross section of the single partial waves are displayed demonstrating that at low energies the S-wave capture dominates, but at 2 MeV the D-waves are no more negligible.

Thus a scattering function containing only the $\alpha + {}^3$He fragmentation yields a very good agreement with the experimental data provided that the bound state function of ^{7}Be satisfies the two above mentioned conditions. This is in accordance with the findings of other recent RGM studies [12-14]).

But in contrast to these, we are able to study the influence of the coupling to inelastic channels like ^{6}Li + p. These closed channels may cause distortion effects in the interaction region and alter the energy dependence of the S-factor, even at astrophysically low energies. Using a scattering function which contains in addition to the open $\alpha + {}^3$He channels closed ^{6}Li + p channels, we calculate the S-factor with

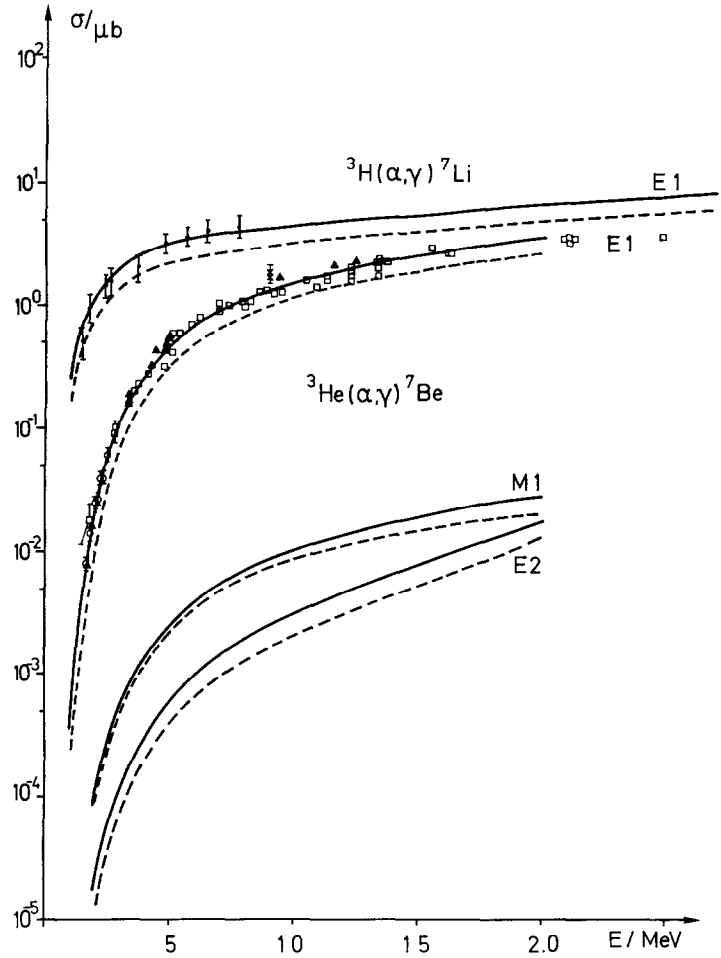

Fig. 2. The E1 capture cross sections for the reactions ^{3}He(α, γ)^{7}Be and ^{3}H(α, γ)^{7}Li (upper curve) together with the data (open squares: ref. [2]), open circles: ref. [3]), full triangles: ref. [4]), crosses: ref. [5]); the data for the lithium capture are from ref. [47]). For the ^{3}He capture reaction also the M1 and E2 cross sections (lower part of the figure) are shown. The full curves give the cross section into the ground state and into the first excited state, the dashed curves only into the ground state.

the same bound state function WF4 for ^{7}Be as before. The result is shown in fig. 3 (dashed line). Using the parametrization of $S(E) = S(0)\exp(aE + bE^2)$ given in ref. [12]) we find $S(0) = 0.53$ keV · b in the single structure calculation and $S(0) = 0.58$ keV · b when we include also the ^{6}Li+p channels. These results agree nicely with other calculations [9-14]) and also with the data [2-5]). Since the calculated phase shifts depend smoothly on energy the above parametrization is well justified.

We consider the difference of 0.05 keV · b between the two calculations as an uncertainty of the calculated astrophysical S-factor at zero energy, because in both cases the calculated phase shifts agree with the existing data at higher energy. The

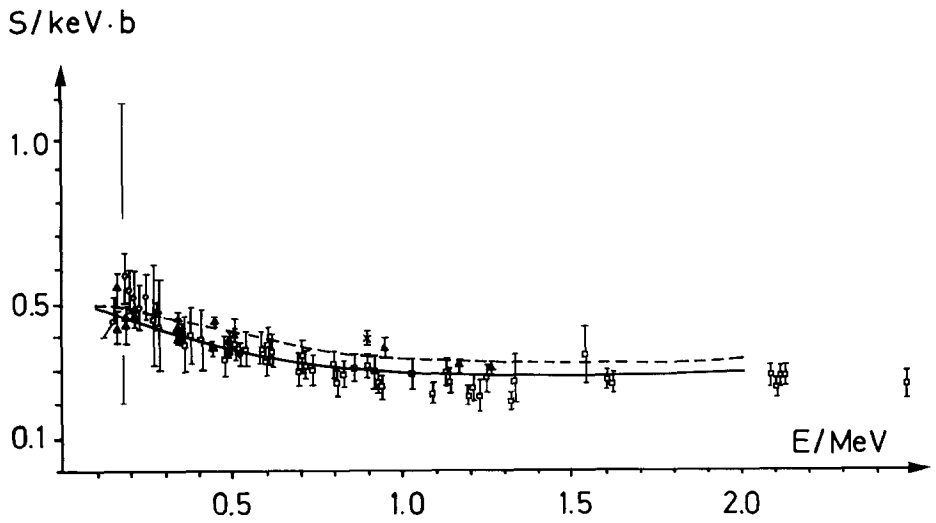

Fig. 3. The calculated astrophysical S-factor for ^{3}He(α, γ)^{7}Be. The data points are the same as in fig. 2. The data of ref. [7]) are not displayed, because they have to be renormalized [55]) and agree essentially with the data shown. The full line is the result of a one-structure (^{4}He+^{3}He) scattering wave function, whereas the dashed curve takes the closed ^{6}Li+p channels into account.

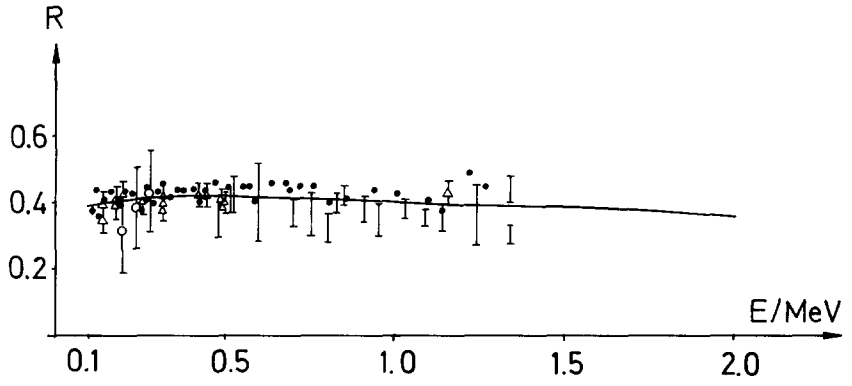

Fig. 4. The branching ratio for the transition into the excited state of ^{7}Be. The data points are the same as in fig. 3 except of the bars without symbol [ref. [2])] and the full circles [ref. [7])].

slightly larger S-factor in the two-structure calculation is due to a less repulsive $^2S_{1/2}$ phase shift.

From these results we can draw the conclusion that the phase shift has to be sufficiently repulsive in order to reproduce the S-factor data and closed ^{6}Li+p channels do not reduce the S-factor at small energies.

For the calculations of the E2 and M1 capture the negative parity scattering functions are needed. Since the $\alpha+^3$He structure gives too a small binding energy, as already indicated in sect. 4.1, the $\frac{3}{2}^-$ and $\frac{1}{2}^-$ bound states of ^{7}Be artificially occur

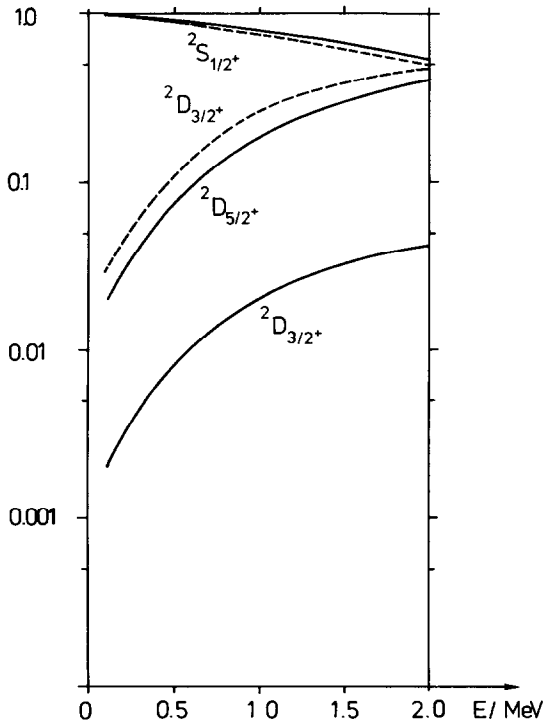

Fig. 5. The relative contribution of the single partial waves for the ground state capture (full line) and for the capture into the first excited state of ^{7}Be (dashed line). The curves are normalized in such a way that the sum of all partial contributions gives 1.

in the one-channel scattering function as resonances (see also ref. [22])). Therefore these phase shifts are not appropriate for the capture calculation. Including closed ^{6}Li+p channels the $\frac{3}{2}^-$ and $\frac{1}{2}^-$ states are bound, as already discussed above, and, hence, the resulting $\frac{3}{2}^-$ and $\frac{1}{2}^-$ phase shifts are repulsive, due to the underlying bound state.

The corresponding E2 and M1 cross section are displayed also in fig. 2. The E2 capture cross section agrees with that of ref. [14]), the M1 cross section, however, is an order of magnitude larger compared to ref. [14]), due to the different $\frac{1}{2}^-$ scattering phase shifts resulting from the different potentials used.

The E1 capture of the mirror reaction ^{3}H(α, γ)^{7}Li is shown in the upper part of fig. 2. It coincides nicely with the latest measurements of ref. [47]). The larger cross section of the reaction ^{3}H(α, γ)^{7}Li compared to ^{3}He(α, γ)^{7}Be just reflects the diminished Coulomb barrier. The S-factor, however, shown in fig. 6 together with the data [47]), is much smaller for this reaction. This is due to the fact that the nucleus ^{7}Li is more strongly bound than ^{7}Be, thus having a minor spatial extension leading to smaller matrix elements. These findings are in agreement with those of ref. [14]). Since the $^2S_{1/2}(^3H+\alpha)$ phase shift is more repulsive than the $^2S_{1/2}(^3He+\alpha)$ phase

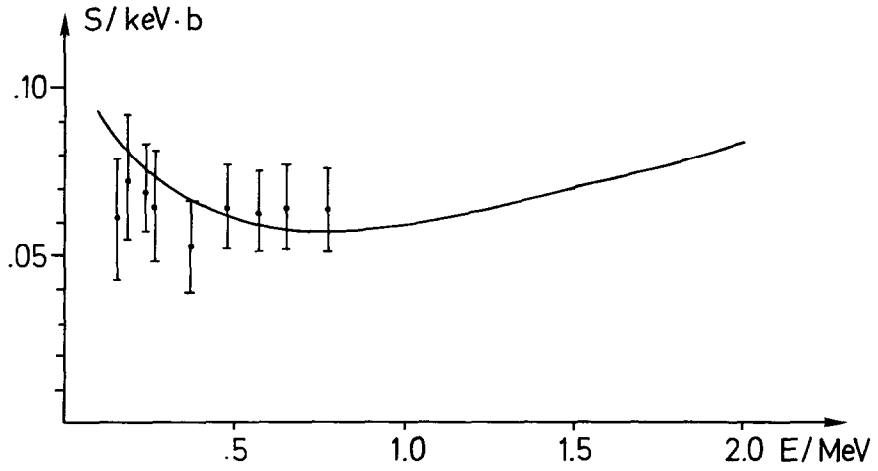

Fig. 6. The S-factor for the capture reaction $^3H(\alpha, \gamma)^7Li$. The data points are from ref. [47]).

shift, the S-factor, however, rises much more steeply with decreasing energy. This might have consequences for the mass fraction of ^{7}Li produced in the early universe. Standard big bang calculations [48]) usually take [49]) $S(0) = 0.064$ keV · b, a value much lower than our calculations indicate. Hence the production of ^{7}Li might be increased appreciably.

4.3. THE POLARISABILITY OF ^{7}Li

We begin the discussion of the tensor polarisability within the closure approximation. Assuming that the intermediate states are degenerated having an energy E, one would identify these states with the giant dipole resonance, whose energy E_D is given by [30])

$$E_D = (40A^{-1/3} + 7.5)\ \text{MeV} \tag{36}$$

resulting in $E_D \approx 28.4$ MeV for ^{7}Li. The evaluation of equation (17) leads then to

$$\tau_{11} = \tau_{11}^{cl}(S_{11}(E1)) = -0.017\ \text{fm}^3,$$

calculated with the bound state function WF1 for ^{7}Li (see appendix 2). Since we are first of all interested in the order of magnitude of τ we mention in passing that all the other bound state wave functions for ^{7}Li given in appendix 2 lead to quite similar results. Furthermore we are discussing only the diagonal term τ_{11} because the non-diagonal quantity τ_{12} has almost the same value due to the similar orbital structure of the bound states with $J^\pi = \frac{3}{2}^-$ and $J^\pi = \frac{1}{2}^-$.

As we have explained in sect. 2, the quantity τ can also be calculated from eq. (18) involving the polarisability α. The result is

$$\tau_{11} = \tau_{11}^{cl}(\alpha) = -0.11\ \text{fm}^3$$

obtained with the same parameters for the wave function and for E_D.

Both results have to be compared with the experimentally established [19,30]) value

$$|\tau_{11}| = |\tau_{12}| = 0.23 \pm 0.06 \text{ fm}^3 .$$

Whereas the calculated $\tau_{11}^{\text{cl}}(S_{11}(\text{E1}))$ is too small by an order of magnitude, the calculated value for $\tau_{11}^{\text{cl}}(\alpha)$ is in accordance with the experimental value, if one realizes that most recent RGM calculations [50]) show positive parity resonances in the energy region between 17 and 23 MeV with different resonance energies for different J^π values, thus indicating a split giant resonance and perhaps invalidating the closure approximation. This low lying giant resonance is also supported by (γ, n) data [51]) which display a broad structured peak in the cross section from 14 to 20 MeV.

Nevertheless the large difference in the calculated values for $\tau_{11}^{\text{cl}}(S_{11}(\text{E1}))$ and $\tau_{11}^{\text{cl}}(\alpha)$ has to be understood. Positive terms only are summed up for the polarisability α, in the case of $S(\text{E1})$, however, the contribution of the intermediate states with $J^\pi = \frac{3}{2}^+$ has the opposite sign to those of $J^\pi = \frac{1}{2}^+$ and $\frac{5}{2}^+$. Consequently the error due to cancellation effects when applying the closure approximation is much larger for $\tau_{11}^{\text{cl}}(S_{11}(\text{E1}))$ than for $\tau_{11}^{\text{cl}}(\alpha)$.

Since, however, the closure approximation might be doubtful altogether, it is much preferable to take the continuous spectrum directly into consideration by applying eqs. (12) to (16) which contain the scattering wave functions. For the bound state of ^{7}Li we use the function WF4 which is the best suited for the topics discussed in sect. 4.1 and 4.2. If we use eqs. (13) and (14) we can write the expression for τ_{if} as an integral which reads

$$\tau_{\text{if}} = \tau_{\text{if}}(S_{\text{if}}(\text{E1})) = \int \rho_{\text{if}}(E)\, \text{d}E . \tag{3}$$

A similar expression is obtained for $\tau_{\text{if}}(\alpha)$.

In fig. 7 the quantities ρ_{11} are displayed as functions of the energy for the three contributing partial waves $J^\pi = \frac{1}{2}^+$, $\frac{3}{2}^+$, and $\frac{5}{2}^+$. The dashed lines are calculated with one-channel ($\alpha + ^3$H) scattering functions, the full lines give the contributions to τ for the two-structure scattering functions which contain in addition to the $\alpha + ^3$H channel ^{6}Li + n channels. The main contribution comes from the partial wave with $J^\pi = \frac{1}{2}^+$ and is concentrated in the energy range between 1 and 3 MeV above the threshold in agreement with ref. [52]). Performing the integration and summing up the partial contributions we obtain $\tau_{11} = -0.084$ fm^3 for the one-channel scattering function and $\tau_{11} = -0.120$ fm^3 for the two-structure case. Without giving the results in detail, we mention that we obtain similar results for τ_{12} and also for the alternative expressions $\tau_{\text{if}}(\alpha)$.

Since there are no positive parity resonances known below 10 MeV [ref. [22])], the tensor polarisability is due to the virtual break-up into the channels $\alpha + ^3$H and ^{6}Li + n. The question however remains where the difference between the calculated and experimental values originates.

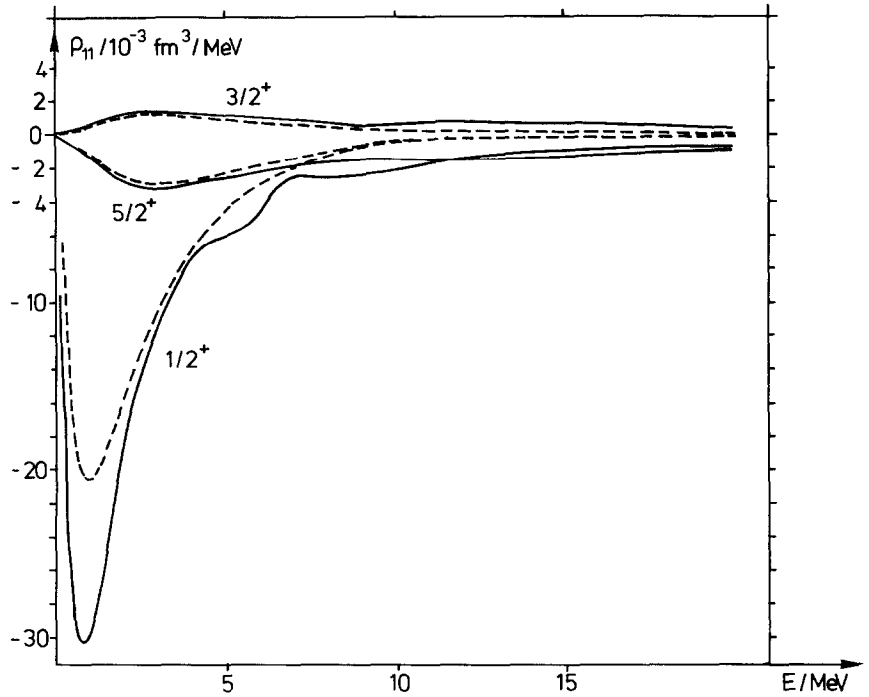

Fig. 7. The integrand of eq. (37) which gives the contribution to the tensor polarisability of ^{7}Li for the single partial waves. The full curves are the result for a two-structure scattering function, whereas the dashed curves take only the ^{4}He+^{3}H waves into consideration.

Since the admixture of the ^{6}Li + n structures increased τ by about 50%, additional structures, like ^{6}Li(3^+) + n or ^{5}He + d might further increase the value. This possibility is supported by the occurrence of positive parity resonances in such channels around 17–23 MeV in recent RGM calculations [50]). The radial parameters used in this calculation do not allow to reproduce the scattering wave function for those large distances needed for the calculation of electromagnetic transition matrix elements. Furthermore the phase shift of the strongly contributing $\frac{1}{2}^+$ channel is not reproduced well enough by the calculation near threshold. Therefore the results of this calculation cannot be used to study the influence of additional structures on the polarisability.

Also a previous analysis [52]) of Coulomb excitation data which takes the radial break-up into the $\alpha + {}^3$H channel into account finds for the polarisability a value quite similar to our calculated one [30]). Furthermore shell model calculations [31,53]) quote similar values for the polarisability, about half of the experimental value deduced in ref. [19]). In these model calculations, however, normalisation factors are necessary in order to reproduce some other electromagnetic properties.

On the other hand fig. 7 demonstrates that the main contribution to τ comes from energies just above the threshold. Thus the adiabatic assumption made in the analysis of the experimental data might not be well founded. The adiabadicity parameter ξ

should fullfil $\xi \gg 1$ and is given by [29])

$$\xi = (E_n - E_i)\eta/2E, \tag{38}$$

where η is the Sommerfeld parameter and E the relative motion energy of the two scattering nuclei. In the underlying experiment [19,30]) we have [54])

$$\xi = 0.69\,(E_n - E_i)/\mathrm{MeV}\,.$$

Using the cluster separation energy of 2.47 MeV we extract from fig. 7 $E_n - E_i \approx$ 3.5 MeV, yielding $\xi \approx 2.4$, a number not far in excess of 1 and much smaller than the one obtained for the giant resonance assumed to be around 28 MeV.

5. Conclusion

In this paper we report on microscopic calculations of the electromagnetic properties of light nuclei. Employing the refined RGM we gave analytical expressions for the matrix elements of the electromagnetic multipole operators in the long wave length limit. Generally this method allows to calculate matrix elements of one-particle operators consisting of gaussian functions, monomials and differential operators.

For the nucleus ^{6}Li we presented results for the electromagnetic moments and reduced transition strengths. In particular we explained the tiny quadrupole moment of ^{6}Li as resulting from interference of different terms in the complicated cluster structure of this nucleus.

In the case of ^{7}Li relatively simple two-cluster wave functions already reproduce reasonably the electromagnetic bound state properties. In order to describe the radiative capture reaction ^{3}He$(\alpha, \gamma)^7$Be at low energies, more complicated bound state functions have to be chosen. The crucial requirements for a calculation of the S-factor are the following. The bound state must have the exact cluster separation energy and the asymptotic behaviour has to meet that of a Whittaker function of this energy. If both these conditions are fulfilled the astrophysical S-factor at zero energy is not altered due to the coupling of the incoming $\alpha + {}^3$He channel with closed ^{6}Li + p channels. Hence, the solar neutrino problem is still with us.

Furthermore we obtained a nice agreement between the calculated cross section and the available data of the mirror reaction ^{3}H$(\alpha, \gamma)^7$Li. In this case, however, the S-factor rises with decreasing energy more strongly than previously extrapolated. This might have consequences concerning the big bang nucleosynthesis calculations.

Finally we studied the polarisability of ^{7}Li in the Coulomb field of a heavy nucleus. We shed some doubts on the validity of the closure approximation. However, a continuum calculation demonstrates that the largest contribution to the polarisability comes from the virtual break-up into the $\alpha + {}^3$H and ^{6}Li + n channels just above the lowest threshold.

Before finishing we want to point out once more that in all calculations the same nucleon-nucleon force was used. Furthermore, no effective charges or g-factors

were applied. Thus we succeeded in describing the electromagnetic properties of the seven-nucleon system in a unified way.

The authors are indebted to D. Fick for various discussions.

Appendix 1

In this appendix we calculate the integral $\Gamma_{L_1M_1\cdots L_NM_N}(i, P, ML)$ which is the coordinate space matrix element of the magnetic orbital operator (3) and is given by [36])

$$\begin{aligned}
&\langle \alpha' l' l' | P\tilde{w}_i(Ll'-l) | \alpha l l \rangle \\
&\quad \sim \Gamma_{L_1M_1\cdots L_NM_N}(i, P, ML) \\
&\quad = \sum_{qq'} (Lq1q'|Ll'-l) e_{q'} \int \mathrm{d}s_1 \cdots \mathrm{d}s_{A-1} \\
&\qquad \times \exp\left(-\sum_{\nu\mu} \rho'_{\nu\mu} s_\nu \cdot s_\mu \right) \left(\prod_{n=n_r}^{N} \mathcal{Y}_{L_nM_n}(Q_n) \right) \mathcal{Y}_{Lq}(Q_{N+1}) \\
&\qquad \times \left(\sum_{k=1}^{A-1} J_{kP(i)} \nabla_{s_k} \right) \exp\left(-\sum_{\nu\mu} \rho''_{\nu\mu} s_\nu \cdot s_\mu \right) \left(\prod_{n=1}^{n_r-1} \mathcal{Y}_{L_nM_n}(Q_n) \right) . \qquad \text{(A.1)}
\end{aligned}$$

Proceeding to the generating function (25) of the spherical harmonics we arrive at

$$\begin{aligned}
&I(i, P, ML, a_1, b_1, \ldots, a_{N+1}, b_{N+1}) \\
&\quad = \sum_{qq'} (Lq1q'|Ll'-l) e_{q'} \\
&\qquad \times \int \mathrm{d}s_1 \cdots \mathrm{d}s_{A-1} \exp\left[-\sum_{\nu\mu} \rho'_{\nu\mu} s_\nu \cdot s_\mu + \sum_{n=n_r}^{N+1} a_n \Lambda(b_n) \cdot Q_n \right] \\
&\qquad \times \left(\sum_{k=1}^{A-1} J_{kP(i)} \nabla_{s_k} \right) \exp\left[-\sum_{\nu\mu} \rho''_{\nu\mu} s_\nu \cdot s_\mu + \sum_{n=1}^{n_r-1} a_n \Lambda(b_n) \cdot Q_n \right] . \qquad \text{(A.2)}
\end{aligned}$$

The vectors $\Lambda(b_n)$ are defined in eq. (26). The expansion of the exponentials in powers of a_n and b_n yields

$$\begin{aligned}
&I(i, P, ML, a_1, b_1, \ldots, a_{N+1}, b_{N+1}) \\
&\quad = \sum_{qq'} (Lq1q'|Ll'-l) e_{q'} \\
&\qquad \times \sum_{l_1 m_1 \cdots l_{N+1} m_{N+1}} \prod_{n=1}^{N+1} (C_{l_n m_n} / l_n!) a_n^{l_n} b_n^{l_n - m_n} \theta_{l_1 m_1 \cdots l_{N+1} m_{N+1}} \qquad \text{(A.3)}
\end{aligned}$$

giving the desired integrals

$$\Gamma_{L_1M_1\cdots L_NM_N}(i, P, ML) = \sum_{qq'} (Lq1q'|Ll'-l) e_{q'} \cdot \theta_{L_1M_1\cdots L_NM_N L-1q} . \qquad \text{(A.4)}$$

On the other side, the differential operator in eq. (A.2) acts on the functions to the right, yielding

$$
\begin{aligned}
&I(i, P, ML, a_1, \ldots, b_{N+1}) \\
&\quad = \sum_{qq'} (Lq1q'|Ll'-l) e_{q'} \\
&\qquad \times \int \mathrm{d}\boldsymbol{s}_1 \cdots \mathrm{d}\boldsymbol{s}_{A-1} \exp\left[-\sum_{\nu\mu} \rho_{\nu\mu} \boldsymbol{s}_\nu \cdot \boldsymbol{s}_\mu + \sum_{n=1}^{N+1} a_n \boldsymbol{\Lambda}(b_n) \cdot \boldsymbol{Q}_n \right] \\
&\qquad \times \left\{ \sum_{k=1}^{A-1} J_{kP(i)} \left[-\sum_{\mu=1}^{A-1} (\rho''_{k\mu} + \rho''_{\mu k}) \boldsymbol{s}_\mu + \sum_{n=1}^{n_r-1} a_n \boldsymbol{\Lambda}(b_n) \xi_{nk} \right] \right\} . \qquad \text{(A.5)}
\end{aligned}
$$

Here the exponentials have been put together according to $\rho_{\nu\mu} = \rho'_{\nu\mu} + \rho''_{\nu\mu}$ and the inter-cluster vectors $\boldsymbol{Q}_n$ have been expressed in terms of Jacobi coordinates

$$
\boldsymbol{Q}_n = \sum_{\mu=1}^{A-1} \xi_{n\mu} \boldsymbol{s}_\mu \qquad (n = 1, \ldots, N+1) .
$$

The quadratic form $\rho_{\nu\mu}$ has to be diagonalized now with the relations

$$
\begin{aligned}
\boldsymbol{s}_\mu &= \sum_{\lambda=\mu}^{A-1} T_{\mu\lambda} \boldsymbol{t}_\lambda \qquad (\mu = 1, \ldots, A-1) , \\
T_{\lambda\lambda} &= 1 \qquad (\lambda = 1, \ldots, A-1) , \\
\sum_{\nu\mu}^{A-1} \rho_{\nu\mu} \boldsymbol{s}_\nu \cdot \boldsymbol{s}_\mu &= \sum_{\lambda=1}^{A-1} \beta_\lambda \boldsymbol{t}_\lambda^2 , \\
\boldsymbol{Q}_n &= \sum_{\mu=1}^{A-1} P_{n\mu} \boldsymbol{t}_\mu . \qquad \text{(A.6)}
\end{aligned}
$$

Applying these transformations we obtain

$$
\begin{aligned}
&I(i, P, ML, a_1, \ldots, b_{N+1}) \\
&\quad = \sum_{qq'} (Lq1q'|Ll'-l) e_{q'} \\
&\qquad \times \int \mathrm{d}\boldsymbol{t}_1 \cdots \mathrm{d}\boldsymbol{t}_{A-1} \exp\left[-\sum_{\lambda=1}^{A-1} \left(\beta_\lambda t_\lambda^2 - \sum_{n=1}^{N+1} a_n P_{n\lambda} \boldsymbol{\Lambda}(b_n) \cdot \boldsymbol{t}_\lambda \right) \right] \\
&\qquad \times \left\{ \sum_{k=1}^{A-1} J_{kP(i)} \left[-\sum_{\lambda=\mu} (\rho''_{k\mu} + \rho''_{\mu k}) T_{\mu\lambda} \boldsymbol{t}_\lambda + \sum_{n=1}^{n_r-1} a_n \boldsymbol{\Lambda}(b_n) \xi_{nk} \right] \right\} . \qquad \text{(A.7)}
\end{aligned}
$$

The integrals in eq. (A.7) can be evaluated straightforwardly. But in order to demonstrate the structure of the integrals, we introduce the abbreviation

$$
\boldsymbol{C}_\lambda = \sum_{n=1}^{N+1} a_n \boldsymbol{\Lambda}(b_n) P_{n\lambda} \qquad \text{(A.8)}
$$

and find

$$
\begin{aligned}
&I(i, P, ML, a_1, \ldots, b_{N+1}) \\
&\quad = \sum_{qq'} (Lq1q'|Ll'-l)e_{q'} \\
&\qquad \times \left\{ \sum_{k=1}^{A-1} J_{kP(i)} \left[- \sum_{\lambda \geqslant \mu} (\rho''_{k\mu} + \rho''_{\mu k}) T_{\mu\lambda} \nabla_{c_\lambda} + \sum_{n=1}^{n_r-1} a_n \Lambda(b_n) \xi_{nk} \right] \right\} \\
&\qquad \times \int \mathrm{d}t_1 \cdots \mathrm{d}t_{A-1} \exp\left(- \sum_{k=1}^{A-1} \beta_k t_k^2 + \sum_{k=1}^{A-1} c_k \cdot t_k \right)
\end{aligned} \tag{A.9}
$$

where the polynomial in the integral (A.7) has been substituted by the differential operator acting on the integral as common in statistical mechanics.

The integration is now performed with the method of completing squares. The result is

$$
\begin{aligned}
&I(i, P, ML, a_1, \ldots, b_{N+1}) \\
&\quad = \sum_{qq'} (Lq1q'|Ll'-l)e_{q'} \\
&\qquad \times \left\{ \sum_{n=1}^{N+1} K_n a_n \Lambda(b_n) \right\} \cdot I(a_1, b_1, \ldots, a_{N+1}, b_{N+1}) ,
\end{aligned} \tag{A.10}
$$

where $I(a_1, b_1, \ldots, a_{N+1}, b_{N+1})$ is a normlike generating integral, defined in eq. (28), and the K_n are given by

$$
K_n = \sum_{k=1}^{A-1} J_{kP(i)} \left[- \sum_{\lambda \geqslant \mu} (\rho''_{k\mu} + \rho''_{\mu k}) T_{\mu\lambda} P_{n\lambda} / 2\beta_\lambda + \theta(n_r - 1 - n) \xi_{nk} \right]. \tag{A.11}
$$

(θ is the Heavyside function.) Eq. (A.10) has to be expanded in powers of a_n and b_n. This expansion is that one of the norm integrals multiplied by the expression in curly brackets. The single a_n leads to a reduction of L_n to $L_n - 1$, whereas the b_n dependence of Λ (see eq. (26) leads to modified M_n values, yielding the desired integrals

$$
\begin{aligned}
&\Gamma_{L_1 M_1 \cdots L_N M_N}(i, P, ML) \\
&\quad = \sum_{n=1}^{N+1} K_n (L_n / C_{L_n M_n}) \\
&\qquad \times \{ \sqrt{2}\, C_{L_n - 1 M_n + 1}(Ll' - l - 111|Ll'-l) \Gamma_{L_1 M_1 \cdots L_n - 1 M_n + 1 \cdots L_N M_N Ll' - l - 1} \\
&\qquad - 2 C_{L_n - 1 M_n}(Ll' - l10|Ll'-l) \Gamma_{L_1 M_1 \cdots L_n - 1 M_n \cdots L_N M_N Ll' - l} \\
&\qquad + \sqrt{2}\, C_{L_n - 1 M_n - 1}(Ll' - l + 11 - 1|Ll'-l) \Gamma_{L_1 M_1 \cdots L_n - 1 M_n - 1 \cdots L_N M_N Ll' - l + 1} \} .
\end{aligned} \tag{A.12}
$$

Appendix 2

Here we give details of the bound state functions used for ^{6}Li, ^{7}Li, and ^{7}Be. For the lowest $T=0$ states of ^{6}Li we use the three-cluster wave function

$$\psi^{J^\pi}(^6\mathrm{Li}) = \mathscr{A}\left\{\exp\left[-\tfrac{1}{4}\beta \sum_{1\leqslant i<j\leqslant 4}(\boldsymbol{r}_i-\boldsymbol{r}_j)^2-\gamma \boldsymbol{s}_4^2\right]\right.$$
$$\left.\times \sum_{n=1}^{2}\sum_{\substack{l_1,l_2=0,2\\ L}} c_n^{l_1 l_2 L}\exp(-\delta_n \boldsymbol{s}_5^2)[[\mathscr{Y}_{l_1}(\boldsymbol{s}_4)\otimes\mathscr{Y}_{l_2}(\boldsymbol{s}_5)]^L\otimes\Xi^1]^J\right\}, \quad \text{(A.13)}$$

where $\boldsymbol{s}_4$ and $\boldsymbol{s}_5$ denote the cluster-relative Jacobi coordinates between the neutron and the proton resp. between the α and the deuteron, and Ξ^1 is the spin-isospin function with $S=1$. The width parameters which in the following are all given in units of fm^{-2} are $\beta=0.2838$, $\gamma=0.3554$, $\delta_1=0.1139$, and $\delta_2=0.02437$. The coefficients $c_n^{l_1 l_2 L}$ are given in table 3.

The two-cluster functions for the seven-nucleon bound states are

$$\psi^{J^\pi}(A=7) = \mathscr{A}\left\{\sum_{m=1}^{M} c_m \exp\left[-\tfrac{1}{4}\beta_m \sum_{1\leqslant i<j\leqslant 4}(\boldsymbol{r}_i-\boldsymbol{r}_j)^2-\tfrac{1}{3}\gamma_m \sum_{5\leqslant i<j\leqslant 7}(\boldsymbol{r}_i-\boldsymbol{r}_j)^2-\delta_m \boldsymbol{s}_6^2\right]\right.$$
$$\left.\times[\mathscr{Y}_1(\boldsymbol{s}_6)\otimes\Xi^{1/2}]^J\right\}, \quad \text{(A.14)}$$

where $\boldsymbol{s}_6$ is the cluster-relative Jacobi coordinate between the α and the ^{3}He/^{3}H and $\Xi^{1/2}$ denotes the spin-isospin function with $S=\frac{1}{2}$. For the wave functions WF1,

TABLE 3

The coefficients $c_n^{l_1 l_2 L}$ in units of 10^{-4} for ^{6}Li together with the calculated and experimental excitation energies of the $T=0$ states

J^π	1^+	3^+	2^+	1^{+*}
c_1^{000}	69.622			0.29966
c_2^{000}	27.322			1.2251
c_1^{202}	4.7790	−8.4509	3.5968	0.28749
c_2^{202}	3.6780	0.71186	−0.33977	0.12083
c_1^{022}	0.92754	10.183	−4.8622	1.0048
c_2^{022}	−0.042680	0.29574	−0.71790	0.89367
c_1^{220}	0.27847			0.14195
c_2^{220}	−0.0040572			0.045597
c_1^{221}	0.29735		0.38212	0.089022
c_2^{221}	−0.0067814		0.021986	0.069851
c_1^{222}	−0.15444	0.10694	0.49293	0.038474
c_2^{222}	−0.00031924	0.0065953	0.047657	0.061432
c_1^{223}		0.50698	0.42532	
c_2^{223}		0.015740	0.062397	
c_1^{224}		1.2078		
c_2^{224}		0.028144		
E_{exc}	0	3.32	4.85	5.37
$E_{\mathrm{exc}}^{\mathrm{exp}}$ (ref. [40])	0	2.185	4.31	5.65

WF2, and WF3 we use the same internal widths which for the α are taken as $\beta_m = 0.2846$ $(m = 1, \ldots, M)$. For the wave functions WF1 and WF2 which contain only one gaussian in the relative motion the ^{3}He width parameters are $\gamma_1 = 0.2760$ and $\gamma_2 = 0.1057$. For WF3 which consists of four gaussians in the relative motion the internal ^{3}He widths are $\gamma_1 = \cdots = \gamma_4 = 0.2760$ and $\gamma_5 = \cdots = \gamma_8 = 0.1057$. The radial widths parameters δ_m and the coefficients c_m are given in table 4.

TABLE 4

The parameters of the wave functions WF1 for ^{7}Li and ^{7}Be, and WF3 for ^{7}Li

	WF1 (WF2)				
m	δ_m	$10^4 c_m(^7\mathrm{Li}(\frac{3}{2}^-))$	$10^4 c_m(^7\mathrm{Li}(\frac{1}{2}^-))$	$10^4 c_m(^7\mathrm{Be}(\frac{3}{2}^-))$	$10^4 c_m(^7\mathrm{Be}(\frac{1}{2}^-))$
1	0.0624 (0.0411)	1.3088	1.2888 (0.6438)	1.2896	1.2690
2	0.0624 (0.0411)	0.10669	0.11433 (0.07788)	0.11404	0.12186
	WF3				
m	$\delta_m(^7\mathrm{Li})$	$10^4 c_m(^7\mathrm{Li}(\frac{3}{2}^-))$	$10^4 c_m(^7\mathrm{Li}(\frac{1}{2}^-))$		
1	0.1835	3.4913	1.4703		
2	0.0591	0.60552	0.62185		
3	0.0193	0.051962	0.068619		
4	0.006	0.00026448	0.0037011		
5	0.1835	−0.76417	−0.68178		
6	0.0591	0.10644	0.087871		
7	0.0193	0.0092190	0.014860		
8	0.006	0.00012049	0.00060469		

The values in brackets correspond to the excited state of ^{7}Li for the wave function WF2.

The wave function WF4 which consists of an superposition of an $\alpha + {}^3\mathrm{H}({}^3\mathrm{He})$ and a three-cluster ^{6}Li+n(p) fragmentation is given by

$$\begin{aligned}\psi^{J^\pi}(A=7) = \mathscr{A}\Bigg\{\Bigg[\sum_{m=1}^{2} d_m \exp\Bigg(-\tfrac{1}{4}\beta_m \sum_{1\leqslant i<j\leqslant 4}(\boldsymbol{r}_i-\boldsymbol{r}_j)^2 - \tfrac{1}{3}\gamma_m \sum_{5\leqslant i<j\leqslant 7}(\boldsymbol{r}_i-\boldsymbol{r}_j)^2\Bigg)\Bigg] \\ \times\Bigg(\sum_{n=1}^{4} c_n \exp(-\delta_n \boldsymbol{s}_6^2)\Bigg)[\mathscr{Y}_1(\boldsymbol{s}_6)\otimes \Xi^{1/2}]^J \\ + \exp\Bigg[-\tfrac{1}{4}\beta' \sum_{1\leqslant i<j\leqslant 4}(\boldsymbol{r}_i-\boldsymbol{r}_j)^2 - \tfrac{1}{2}\gamma'(\boldsymbol{r}_s-\boldsymbol{r}_6)^2 - \varepsilon' \boldsymbol{s}_5'^2\Bigg] \\ \times\Bigg(\sum_{m=5}^{6} c_m \exp(-\delta_m \boldsymbol{s}_6'^2)[\mathscr{Y}_0(\boldsymbol{s}_5')\mathscr{Y}_1(\boldsymbol{s}_6')\otimes \Xi^{3/2}]^J \\ + \sum_{m=7}^{8} c_m \exp(-\delta_m \boldsymbol{s}_6'^2)[\mathscr{Y}_0(\boldsymbol{s}_5')\mathscr{Y}_1(\boldsymbol{s}_6')\otimes \Xi^{1/2}]^J\Bigg)\Bigg\}. \qquad \text{(A.15)}\end{aligned}$$

Here $\boldsymbol{s}_6$ is the Jacobi relative coordinate of the $\alpha + {}^3\mathrm{H}({}^3\mathrm{He})$ fragmentation, and $\boldsymbol{s}_5'$ and $\boldsymbol{s}_6'$ are the Jacobi relative coordinates of the structure ^{6}Li+n(p).

TABLE 5

The widths δ_m and the coefficients c_m ($m = 1, \ldots, 8$) of the wave function WF4 for ^{7}Li and ^{7}Be

	^{7}Li ($\frac{3}{2}^-$)		^{7}Li ($\frac{1}{2}^-$)		^{7}Be ($\frac{3}{2}^-$)		^{7}Be ($\frac{1}{2}^-$)	
m	δ_m	$c_m \cdot 410^4$	δ_m	$c_m \cdot 10^4$	δ_m	$c_m \cdot 10^4$	δ_m	$c_m \cdot 10^4$
1	0.3020	29.03	0.2446	19.38	0.2972	27.64	0.2451	18.53
2	0.0725	−4.325	0.0374	−1.754	0.0713	−3.991	0.0353	−1.609
3	0.0251	−0.5412	0.008	−0.0193	0.0243	−0.5559	0.008	−0.02437
4	0.007	−0.002734	-	0	0.007	−0.006056	-	0
5	0.3019	6.457	0.3019	1.525	0.2971	−5.527	0.2971	−1.231
6	0.0524	0.1437	0.0524	0.0710	0.0517	−0.1310	0.0517	−0.651
7	0.3019	−0.7637	0.3019	−7.998	0.2971	0.6916	0.2971	6.724
8	0.0524	−0.4356	0.0524	−0.7515	0.0517	0.4539	0.0517	0.7305

TABLE 6

The coefficients of the effective nucleon-nucleon potential

$A_c^{1+,1} = -692.60$	$A_c^{3+,1} = -510.32$	$B_c^{1+,1} = B_c^{3+,1} = 7.1199$
$A_c^{1+,2} = 904.72$	$A_c^{3+,2} = 681.06$	$B_c^{1+,2} = B_c^{3+,2} = 4.8092$
$A_c^{1+,3} = -77.031$	$A_c^{3+,3} = -8.004$	$B_c^{1+,3} = B_c^{3+,3} = 0.6409$
$A_c^{1+,4} = -14.843$	$A_c^{3+,4} = -87.917$	$B_c^{1+,4} = B_c^{3+,4} = 0.4430$
$A_{LS}^{3+,1} = 214.585$	$A_{LS}^{3-,1} = -262.507$	$B_{LS}^{3+,1} = B_{LS}^{3-,1} = 1.7888$
$A_{LS}^{3+,2} = -0.811$	$A_{LS}^{3-,2} = -25.772$	$B_{LS}^{3+,2} = B_{LS}^{3-,2} = 1.2851$
$A_T^{3+,1} = -102.692$	$A_T^{3-,1} = -8.129$	$B_T^{3+,1} = B_T^{3-,1} = 1.0942$
$A_T^{3+,2} = -2.740$	$A_T^{3-,2} = 25.105$	$B_T^{3+,2} = B_T^{3-,2} = 0.8364$
$A_T^{3+,3} = -1.863$	$A_T^{3-,3} = 0.613$	$B_T^{3+,3} = B_T^{3-,3} = 0.2380$

The width parameters B are given in fm^{-2} and the strength parameters A in MeV. The indices c, LS and T denote the central, spin-orbit and tensor parts, respectively.

The internal widths $\beta_1 = \beta_2 = 0.2846$, $\gamma_1 = 0.2760$ and $\gamma_2 = 0.1057$ are combined with the coefficients $d_1 = 0.1544$ and $d_2 = 0.03014$ for ^{7}Li and $d_1 = 0.1501$ and $d_2 = 0.03120$ for ^{7}Be. The internal widths for the second fragmentation are $\beta' = 0.2863$, $\gamma' = 0.2398$ and $\varepsilon' = 0.0972$ for ^{7}Li and $\varepsilon' = 0.0916$ for ^{7}Be. The widths for the relative motion δ_m and the coefficients c_m are given in table 5. The calculated cluster separation energies of the ground and first excited state of ^{7}Li are 2.44 MeV and 2.14 MeV compared to the experimental values [40]) of 2.47 MeV and 1.99 MeV. For ^{7}Be the calculated energies are 1.60 MeV and 1.19 MeV compared to [40]) 1.59 MeV and 1.16 MeV.

Appendix 3

The effective nucleon-nucleon potential employed is derived from a realistic NN potential [34]). Following the notation of ref. [34]), the potential is taken as

$$V = V^{1+}P^{1+} + V^{1-}P^{1-} + V^{3+}P^{3+} + V^{3-}P^{3-}. \tag{A.16}$$

The operators P^{1+}, P^{1-}, P^{3+} and P^{3-} are projection operators for the singlet-even, singlet-odd, triplet-even and triplet-odd states, respectively. The central potential contains only even contributions, whereas the spin–orbit and tensor potential consist of even and odd parts. The radial dependence is given by sums of gaussian functions; for instance [34])

$$V_c^{1+}(r) = \sum_{i=1}^{4} A_c^{1+,i} \exp\left(-B_c^{1+,i} r^2\right), \tag{A.17}$$

where the index c characterizes the central part. The coefficients A and B are given in table 6. This potential presupposes the use of Jastrow-correlation functions in the form [32]) of $f(r) = 1 - 0.6 \exp(-3\ \mathrm{fm}^{-2} r^2)$ for the kinetic energy only. This potential has been extensively used for scattering calculations in various nuclei [23]). For the systems with 6 and 7 nucleons the spin–orbit part is multiplied by a factor 2.0 in order to improve the position of resonances [22]).

References

1) J.N. Bahcall, W.F. Huebner, S.I. Lubow, P.D. Parker and R.K. Ulrich, Rev. Mod. Phys. **54** (1982) 767
2) P.D. Parker and R.W. Kavanagh, Phys. Rev. **131** (1963) 2578
3) K. Nagatani, M.R. Dwarakanath and D. Ashery, Nucl. Phys. **A128** (1969) 325
4) J.L. Osborne, C.A. Barnes, R.W. Kavanagh, R.M. Kremer, G.J. Mathews, J.L. Zyskind, P.D. Parker and A.J. Howard, Phys. Rev. Lett. **48** (1982) 1664 and Nucl. Phys. **A419** (1984) 115
5) R.G.H. Robertson, P. Dyer, T.J. Bowles, R.E. Brown, N. Jarmie and E.J. Maggiore, Phys. Rev. **C27** (1983) 11
6) T.K. Alexander, G.C. Ball, W.N. Lenard, H. Geissel and H.-B. Mak, Nucl. Phys. **A427** (1984) 526
7) H. Kräwinkel, A.W. Becker, L. Buchmann, J. Görres, K.U. Klettner, W.E. Kieser, R. Santo, P. Schmalbrock, H.P. Trautvetter, A. Vlieks, C. Rolfs, J.W. Hammer, R.E. Azuma and W.S. Rodney, Z. Phys. **A304** (1982) 307
8) T.A. Tombrello and P.D. Parker, Phys. Rev. **131** (1963) 2582
9) B.T. Kim, T. Izumoto and K. Nagatani, Phys. Rev. **C23** (1981) 33
10) R.D. Williams and S.E. Koonin, Phys. Rev. **C23** (1981) 2773
11) B. Buck, R.A. Baldock and J.A. Rubio, J. of Phys. **G11** (1985) L11
12) H. Walliser, H. Kanada and Y.C. Tang, Nucl. Phys. **A419** (1984) 133
13) Q.K.K. Liu, H. Kanada and Y.C. Tang, Phys. Rev. **C23** (1981) 645
14) T. Kajino and A. Arima, Phys. Rev. Lett. **52** (1984) 739, and T. Kajino, Proc. INS-RIKEN Intern. Symp. on Heavy ion physics, Mt. Fuji, 1984
15) O. Häusser, A.B. McDonald, T.K. Alexander, A.J. Ferguson and R.E. Warner, Nucl. Phys. **A212** (1973) 613
16) A. Bamberger, G. Jansen, B. Povh, D. Schwalm and U. Smilansky, Nucl. Phys. **A194** (1972) 193
17) W.J. Vermeer, M.T. Esat, M.P. Fewell, R.H. Spear, A.M. Baxter and S.M. Burnett, Phys. Lett. **138B** (1984) 365; Austral. J. Phys. **37** (1984) 273
18) P. Egelhof, W. Dreves, K.-H. Möbius, E. Steffens, G. Tungate, P. Zupranski, D. Fick, R. Böttger and F. Roesel, Phys. Rev. Lett. **44** (1980) 1380
19) A. Weller, P. Egelhof, R. Caplar, O. Karban, D. Krämer, K.-H. Möbius, Z. Moroz, K. Rusek, E. Steffens, G. Tungate, K. Blatt, I. König and D. Fick, Phys. Rev. Lett. **55** (1985) 480
20) S. Green, Phys. Rev. **A4** (1971) 251
21) D. Sundholm, P. Pyykkö, L. Laaksonen and A.J. Sadlej, Chem. Phys. Lett. **112** (1984) 1
22) H.M. Hofmann, T. Mertelmeir and W. Zahn, Nucl. Phys. **A410** (1983) 208
23) H.M. Hofmann, Nucl. Phys. **A416** (1984) 363c

24) A. Messiah, Quantum mechanics (North-Holland, Amsterdam, 1961)
25) H.J. Rose and D.M. Brink, Rev. Mod. Phys. **39** (1967) 306
26) A.J.F. Siegert, Phys. Rev. **52** (1937) 778
27) B.F. Gibson, Nucl. Phys. **A416** (1984) 503c
28) A.R. Edmonds, Angular momentum in quantum mechanics (Princeton University Press, Princeton, 1960)
29) K. Alder and A. Winther, Electromagnetic excitation (North-Holland, Amsterdam, 1975)
30) A. Weller, dissertation (Marburg, 1984)
31) F.C. Barker, Austral. J. Phys. **35** (1982) 291
32) H.H. Hackenbroich, Z. Phys. **231** (1970) 216
33) H.H. Hackenbroich, Proc. Int. Symp. on present status and novel developments in the nulcear many-body problem, Rome, 1972, ed. F. Calogero and C. Ciofi degli Atti (Editrice Compositori, Bologna, 1973) p. 706
34) H. Eikemeier and H.H. Hackenbroich, Nucl. Phys. **A169** (1971) 407
35) H.M. Hofmann and T. Mertelmeier, Die Berechnung von Matrixelementen im Refined Resonating Group Modell, Interner Bericht (Erlangen, 1984)
36) T. Mertelmeier, dissertation (Erlangen, 1985)
37) M.E. Rose, Elementary theory of angular momentum (Wiley, New York, 1953)
38) A.C. Merchant and N. Rowley, Phys. Lett. **150B** (1984) 35
39) F. Eigenbrod, Z. Phys. **228** (1969) 337
40) F. Ajzenberg-Selove, Nucl. Phys. **A413** (1984) 1
41) C.W. Jager, H. de Vries and C. de Vries, Atomic Data Nucl. Data Tables **14** (1974) 479
42) M. Bernheim and G.R. Bishop, Phys. Lett. **5** (1963) 270
43) G.J.C. Van Niftrik, L. Lapikas, H. de Vries and G. Box, Nucl. Phys. **A174** (1971) 173
44) H. Orth, H. Ackermann and E.W. Otten, Z. Phys. **A273** (1975) 221
45) R.E. Rand, R. Frosch and M.R. Yearian, Phys. Rev. **144** (1966) 859 and Phys. Rev. **148** (1966) 1246
46) H. Walliser and Y.C. Tang, Phys. Lett. **135B** (1984) 344
47) G.M. Griffiths, R.A. Morrow, P.J. Riley and J.B. Warren, Can. J. Phys. **39** (1961) 1397
48) R.V. Wagoner, Ap. J. **179** (1973) 343
49) W.A. Fowler, G.R. Caughlan and B.A. Zimmerman, Ann. Rev. Astr. Ap. **5** (1967) 525
50) M. Herman, H.M. Hofmann and S. Stocker, Verh. DPG (VI) **20** (1985) 560 and to be published
51) R.L. Bramblet, B.L. Berman, M.A. Kelly, J.T. Caldwell and S.C. Fultz, Proc. Int. Conf. on Photonuclear reactions and applications, Asilomar, 1973, ed. B.L. Berman, p. 175
52) U. Smilansky, B. Povh and K. Traxel, Phys. Lett. **38B** (1972) 293
53) J. Gomez-Camacho and M.A. Nagarajan, Daresbury Laboratory, 1985, preprint
54) A. Weller, private communication, 1985
55) C. Rolfs, private communication and to be published